Mode generation and diffraction at the aperture of a waveguide

2005 J. Phys. A: Math. Gen. 38 2701

(http://iopscience.iop.org/0305-4470/38/12/012)

INSTITUTE OF PHYSICS PUBLISHING JOURNAL OF PHYSICS A: MATHEMATICAL AND GENERAL

J. Phys. A: Math. Gen. **38** (2005) 2701–2713 doi:10.1088/0305-4470/38/12/012

Mode generation and diffraction at the aperture of a waveguide

Ian Thompson[1], **Richard Tew**[1] **and Christos Christopoulos**[2]

[1] Division of Applied Mathematics, School of Mathematical Sciences, University of Nottingham, University Park, Nottingham NG7 2RD, UK
[2] George Green Institute for Electromagnetics Research, School of Electrical and Electronic Engineering, University of Nottingham, University Park, Nottingham NG7 2RD, UK

E-mail: richard.tew@nottingham.ac.uk

Received 25 October 2004, in final form 12 January 2005
Published 9 March 2005
Online at stacks.iop.org/JPhysA/38/2701

Abstract
Using a combination of exact results from diffraction theory and the method of images, we calculate to leading order in the high-frequency limit, the modes excited within a waveguide comprising a pair of semi-infinite parallel half-planes when a wave strikes its aperture. We consider several types of incident field, and the calculation that we present does not rely on any approximations (such as stationary phase or steepest descent integral evaluations) and is somewhat less involved than methods in the existing literature that do so. Furthermore, it permits the consideration of situations in which 'Fresnel' regions propagate within the guide, and of more complicated geometries, whilst retaining its straightforward nature.

PACS numbers: 42.15.Dp, 42.25.Fx, 42.82.Et, 43.20.+g

1. Introduction

It is generally accepted that the geometrical theory of diffraction (GTD) [1] is the standard method for calculating asymptotic expansions of solutions to problems involving the radiation, scattering and diffraction of linear, high-frequency waves in non-separable domains. For a comprehensive review of the theory behind this method and of numerous important applications, see [2]; we also note that an account of a similar approach to a class of nonlinear problems is presented by Anile *et al* [3] and Prasad [4]. For problems involving the scattering of a prescribed incoming field by an obstructing boundary, be it acoustic, electromagnetic or elastodynamic in nature, the underlying idea is to decompose the incident wave into its constituent 'rays' (which are everywhere normal to the wave fronts) and then to use the recipes laid out in the aforementioned references to construct a ray description of the scattered field. Often, certain 'diffraction coefficients' within the amplitude profile need to be determined by comparison with exact solutions to appropriate canonical problems, such as diffraction by half-planes, wedges or vertices, for example. The problems considered in the work cited thus far involve, for the most part, unbounded (though possibly semi-infinite) domains. Inside closed, bounded domains, the allowable wave numbers and solutions that can exist are determined via an eigenvalue problem. For convex boundaries, this problem was solved using ray methods by Keller and Rubinow [5].

A half-way-house occurs when there is coupling between propagating modes in a semi-infinite waveguide and external fields in the unbounded domain exterior to the guide. It might be that the modal waves are excited as a result of an external field impinging upon the aperture, or by modes travelling within the guide. Here, diffraction of order $n + 1$ occurs when a ray that has already been diffracted n times strikes one of the sharp edges that form the aperture. Now the field excited within the guide can be expressed as a series of modes via elementary methods [6, 7]. However, the determination of the amplitude coefficients which correctly represent the diffractive effects at the aperture edges is much more difficult; this is what concerns us here. Yee *et al* [8] demonstrated the use of the GTD in two-dimensional problems involving scattering of guided modes at the aperture of such a waveguide. By considering each successive diffraction effect as a source of rays, and using the method of images, an expression for the resulting guided modes was obtained, with each term in the asymptotic expansion of the amplitude coefficients represented by an integral. These coefficients were then approximated using the method of stationary phase. This method is now often referred to as *ray-mode conversion*. By comparing exact results available via the Wiener–Hopf technique for simple geometries [9] with those of Yee *et al*, Bowman [10] later found that latter are correct only for primary and secondary diffraction (i.e. for $n = 1$ and $n = 2$); this issue was subsequently resolved by Boersma [11]. However, one issue that does not appear to have been noticed is that, in calculating the modes generated by the incident field, primary diffraction and specular reflections thereof, Yee *et al* apply two approximations (a ray representation from each source followed by a stationary phase integral evaluation), and yet they still obtain an exact result. Our purpose in this paper is partly to demonstrate how, in problems involving open-ended waveguides formed by half-planes, this calculation may be performed without the need for any of the aforementioned approximations. The only special requirement is that for the given incident field (and in this context a guided mode is equivalent to a pair of plane waves), an exact expression for the field diffracted by a half-plane is available in the form of a Fourier integral. In addition, the procedure that we present may be employed both when the incident field comprises modes propagating within the guide, and also when it impinges upon the aperture externally, thus accounting for situations not previously considered, in which optical shadow boundaries and their associated Fresnel regions are present within the guide; this is not possible using the method of Yee *et al*. The results obtained describe the leading-order behaviour in the high-frequency limit and are therefore particularly useful in applications such as electromagnetism. It should be emphasized that the issue of Fresnel regions occurring within the guide (i.e. beyond the aperture) can only arise when considering primary diffraction. Higher order effects possess optical boundaries that are perpendicular to the half-planes; their contribution to the amplitude coefficients can be determined using the methods of Boersma [11]. Our method can be extended with little effort to account for more complicated geometries, and generally represents a simpler approach to obtaining the leading-order field within the guide than those based on the Wiener–Hopf technique.

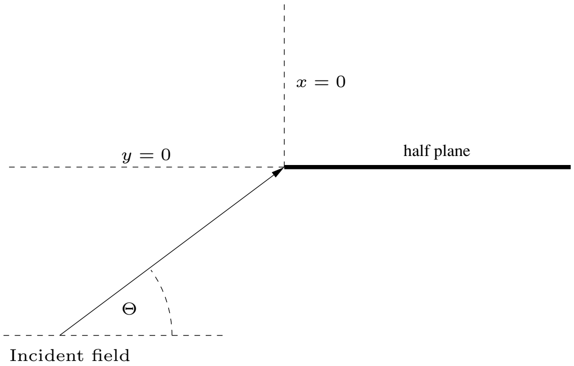

Figure 1. Geometrical configuration.

2. Review of diffraction by a half-plane

In this section, we present a summary of useful results relating to diffraction by a half-plane. At the outset, we take all fields to be time-harmonic; the factor $\mathrm{e}^{-\mathrm{i}\omega t}$ is assumed and omitted throughout. Now, consider a wave $\phi^{\mathrm{i}}(x, y)$ incident at angle $\Theta \in (-\pi, \pi)$ upon the edge of a half-plane that occupies $x > 0$, $y = 0$, for all values of z. If ϕ^{i} is a plane wave, then Θ represents its direction of propagation; on the other hand, if it is a cylindrical wave, then Θ is the angle of elevation of the line joining the source to the edge of the half-plane. In either case, Θ is illustrated in figure 1. Let ϕ represent the resulting scattered field, which satisfies the Helmholtz equation, i.e.

$$(\nabla^2 + k^2)\phi(x, y) = 0.$$

Here, the wave number is defined via $k = \omega/c$, where ω is the angular frequency and c is the wave speed of the medium. The incident wave ϕ^{i} also satisfies the Helmholtz equation, though in the case of a cylindrical wave, a forcing term must be included. The total field is given by

$$\phi^{\mathrm{t}}(x, y) = \phi(x, y) + \phi^{\mathrm{i}}(x, y),$$

and we have either $\phi^{\mathrm{t}} = 0$ or $\frac{\partial \phi^{\mathrm{t}}}{\partial y} = 0$ on the surface of the half-plane for Dirichlet or Neumann conditions, respectively. In the context of acoustics, the Dirichlet condition represents a ‘sound-soft’ boundary, and the Neumann condition a ‘sound-hard’ boundary; see [12] for a further discussion. In addition, it is well known [13] that the solution to any two-dimensional problem arising in electromagnetics, and involving only perfectly conducting (i.e. metal) boundaries, can be constructed from the solutions to the Dirichlet and Neumann problems.

Now, let $\phi^{\mathrm{r}}(x, y)$ represent the specularly reflected field, by which we mean the exact solution to the reflection problem in the event that the obstructing boundary is infinite. This can easily be calculated for any type of incident wave. By definition, $\phi^{\mathrm{i}} + \phi^{\mathrm{r}}$ satisfies the boundary conditions on $y = 0$, $x > 0$. Now, introduce the quantity $\phi'(x, y)$, which consists of $\phi + \phi^{\mathrm{i}}$ on the dark side of the plane and $\phi - \phi^{\mathrm{r}}$ on the lit side. Then ϕ' also satisfies the boundary condition; it represents the total field on the dark side of the plane, and the diffracted field (with no incident or reflected wave) on the lit side. In general, a Fourier integral expression for ϕ' may be obtained via the Wiener–Hopf technique; it has the form

$$\phi'(x, y) = \begin{bmatrix} 1 \\ \mathrm{sgn}(y) \end{bmatrix} \frac{1}{2\pi} \int_{-\infty}^{\infty} \frac{S^{+}(\alpha)}{\gamma^{[\mp]}(\alpha)}\, \mathrm{e}^{-\gamma(\alpha)|y|}\, \mathrm{e}^{-\mathrm{i}\alpha x}\, \mathrm{d}\alpha. \tag{1}$$

Here, a superscript '+' ('−') implies that the function is analytic on and above (below) the contour of integration, and the backslash through the integral indicates that singularity contributions due to the function $S^+(\alpha)$ are to be removed. The precise means by which this is achieved depends upon the incident field; two examples are given below. The upper and lower symbols within square brackets refer to the Dirichlet and Neumann cases, respectively; this convention for field expressions is maintained throughout. The functions $\gamma^\pm$ are defined as

$$\gamma^\pm(\alpha) = \mathrm{e}^{\mp \mathrm{i}\frac{\pi}{4}}(\alpha \pm k)^{1/2}, \tag{2}$$

with $\gamma^\pm(0) = \mathrm{e}^{-\mathrm{i}\pi/4}(k)^{1/2}$, and the branch cuts chosen so as not to cross the real axis. Note that $\gamma^+(\alpha) = \gamma^-(-\alpha)$. These are obtained via a Wiener–Hopf product factorization [9] of

$$\gamma(\alpha) = (\alpha^2 - k^2)^{1/2},$$

with $\gamma(0) = -\mathrm{i}k$. As is conventional, the wave number k is assumed to have a small, positive imaginary part, corresponding to slight decay, and when we write $k^{1/2}$ we refer to the value in the upper-right quadrant of the complex plane. This ensures the convergence of all subsequent integrals; the limit $k \to \mathrm{Re}(k)$ may be applied to the final results as usual.

The form of S^+ depends upon the incident field; singularity contributions from this function yield the reflected field on the lit side of the plane, and $-\phi^{\mathrm{i}}$ on the dark side. For example, for the plane wave

$$\phi^{\mathrm{i}}(x, y) = \mathrm{e}^{\mathrm{i}k(x\cos\Theta + y\sin\Theta)},$$

we have [9]

$$S^+(\alpha) = -\begin{bmatrix} \cos\dfrac{\Theta}{2} \\ \sin\dfrac{\Theta}{2} \end{bmatrix} \mathrm{e}^{\mathrm{i}\pi/4}(2k)^{1/2}(\alpha + k\cos\Theta)^{-1}, \tag{3}$$

and the integral in (1) is to be modified by deforming the contour of integration to pass below $\alpha = -k\cos\Theta$ without including a residue term. If the incident field is generated by a uniform line source of unit strength located at the point $(-X, -Y)$, so that now

$$(\nabla^2 + k^2)\phi^{\mathrm{i}}(x, y) = \delta(x + X)\delta(y + Y),$$

where $\delta(\cdot)$ is the Dirac delta function, then it is not difficult to show that

$$\phi^{\mathrm{i}}(x, y) = -\frac{1}{4\pi}\int_{-\infty}^{\infty} \mathrm{e}^{-\gamma(\alpha)|y+Y|}\,\mathrm{e}^{\mathrm{i}\alpha(x+X)}\,\frac{\mathrm{d}\alpha}{\gamma(\alpha)}, \tag{4}$$

which is a standard integral [9] representing a zeroth-order Hankel function of the first kind, i.e.

$$\phi^{\mathrm{i}}(x, y) = -\frac{\mathrm{i}}{4}H_0^{(1)}\left(k\sqrt{(X + x)^2 + (Y + y)^2}\right). \tag{5}$$

In this case,

$$S^+(\alpha) = \begin{bmatrix} 1 \\ \mathrm{sgn}(Y) \end{bmatrix} \frac{\mathrm{e}^{\mathrm{i}kR}}{4\gamma^{[\pm]}(\alpha)}[w(z_1)[\pm]w(z_2)],$$

where $w(\cdot)$ is the scaled complex error function [14], i.e. $w(z) = \mathrm{e}^{-z^2}\,\mathrm{erfc}(-\mathrm{i}z)$, with

$$z_1(\alpha) = \mathrm{i}\sqrt{R}\left[\cos\frac{\Theta}{2}\gamma^+(\alpha) - \left|\sin\frac{\Theta}{2}\right|\gamma^-(\alpha)\right], \tag{6}$$

and

$$z_2(\alpha) = \mathrm{i}\sqrt{R}\left[\cos\frac{\Theta}{2}\gamma^+(\alpha) + \left|\sin\frac{\Theta}{2}\right|\gamma^-(\alpha)\right]. \tag{7}$$

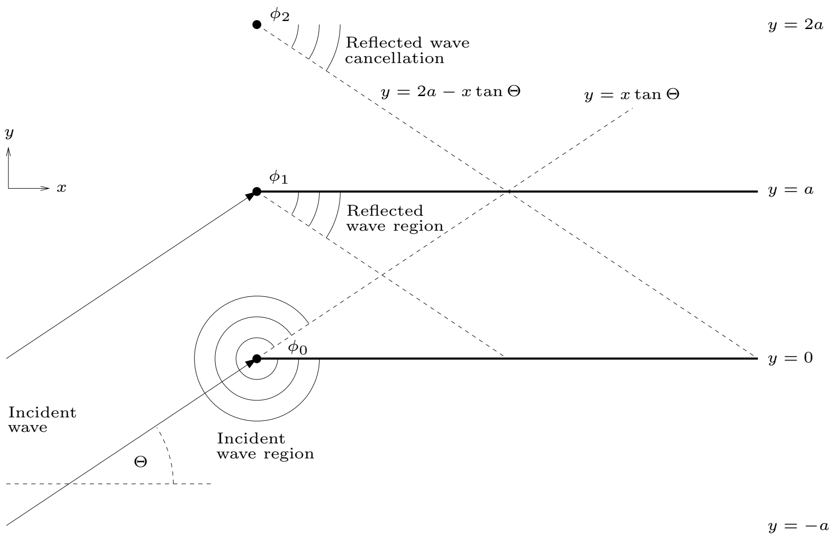

Figure 2. The waveguide, shown with a plane wave incident from free space, along with the wave fields ϕ_0, ϕ_1 and ϕ_2.

Here, R is the distance between the source point in the (x, y) plane and the edge of the half-plane, so that

$$X = R\cos\Theta, \qquad Y = R\sin\Theta.$$

It is not difficult to see that S^+ has no branch point at $\alpha = k$. Furthermore, given that $\Theta \in (-\pi, \pi)$, we can use the definition of the functions $\gamma^{\pm}$ in (2), along with the expansion [14]

$$w(z) \sim \mathrm{i}/(z\sqrt{\pi}) + O(z^{-3/2}), \quad |z| \to \infty, \quad \arg(z) \in \left(-\frac{\pi}{4}, \frac{5\pi}{4}\right), \tag{8}$$

to show that $S^+ \to 0$ as α tends to infinity in the upper half-plane. Now S^+ is derived from an analytic sum factorization [9] of the function S, where

$$S(\alpha) = \begin{bmatrix} 1 \\ \mathrm{sgn}(Y) \end{bmatrix} \frac{1}{2\gamma^{[\pm]}(\alpha)} \mathrm{e}^{-\gamma(\alpha)|Y| - \mathrm{i}\alpha X}. \tag{9}$$

We also have

$$S^-(\alpha) = \begin{bmatrix} 1 \\ \mathrm{sgn}(Y) \end{bmatrix} \frac{\mathrm{e}^{\mathrm{i}kR}}{4\gamma^{[\pm]}(\alpha)} [w(-z_1)[\mp]w(z_2)]. \tag{10}$$

This has no branch point at $\alpha = -k$ and tends to zero as $\alpha \to \infty$ in the lower half-plane. Using the identity [14] $w(z) + w(-z) = 2\,\mathrm{e}^{-z^2}$, we write $S^+ = S - S^-$. The first term gives the specular fields via the integral (4), therefore in this case, the appropriate modification corresponding to the backslash in the integral (1) is the replacement of S^+ with $-S^-$.

3. General construction of the induced waveguide modes

Now consider a waveguide bounded by two half-planes occupying $x > 0$, $y = 0$ and $y = a$. As before, the boundary conditions may require that the total field ϕ^{t} vanishes on the half-planes (Dirichlet case) or that its first y-derivative does so (Neumann case). Suppose that an incident field ϕ^{i} impinges upon the aperture of the guide, see figure 2. Let ϕ_0 represent the *total* field in the absence of the upper half-plane. Primary diffraction by the upper edge is considered below. By definition, this satisfies the boundary conditions at $y = 0$, but not at $y = a$. We must therefore account for the specular reflection of ϕ_0 by the upper half-plane using the method of images. Within the guide, this effect is equivalent to the field

$$\phi_2(x, y) = [\mp]\phi_0(x, 2a - y).$$

Here, the direction of propagation in y has been reversed, and the displacement $2a$ included in the y dependence to give equality at $y = a$. Next, we must account for the specular reflection of ϕ_2 at $y = 0$; this requires a further field which we denote by ϕ_{-2}. It is not difficult to see that

$$\begin{aligned} \phi_{-2}(x, y) &= [\mp]\phi_2(x, -y) \qquad & \phi_4(x, y) &= [\mp]\phi_{-2}(x, 2a - y) \\ &= \phi_0(x, 2a + y) & &= [\mp]\phi_0(4a - y), \end{aligned}$$

etc. Continuing this process *ad infinitum,* we find that the field within the guide due to the incident field, primary diffraction at the lower edge (0, 0), and specular reflections thereof is given in terms of ϕ_0 by

$$\phi^{1}(x, y) = \sum_{j=-\infty}^{0} \phi_0(x, y - 2ja)[\mp]\sum_{j=1}^{\infty} \phi_0(x, 2ja - y). \tag{11}$$

The series expansion of ϕ^1 in (11) clearly satisfies the boundary conditions on both walls of the guide. Since we are only concerned with $0 \leqslant y \leqslant a$, (11) may also be written as the Fourier series

$$\phi^{1}(x, y) = \sum_{m=0}^{\infty} A^1_m(x) \begin{bmatrix}\sin\\ \cos\end{bmatrix} \left(\frac{m\pi y}{a}\right), \tag{12}$$

from which the modal form of this wave field is becoming evident. By Fourier inversion, it then follows that

$$\begin{aligned} A_m(x)^1 = \frac{1}{(1+\delta_{m0})a} \Bigg\{ &\sum_{j=-\infty}^{0} \int_0^{2a} \phi_0(x, y - 2ja) \begin{bmatrix}\sin\\ \cos\end{bmatrix} \left(\frac{m\pi y}{a}\right) \mathrm{d}y \\ &[\mp]\sum_{j=1}^{\infty} \int_0^{2a} \phi_0(x, 2ja - y) \begin{bmatrix}\sin\\ \cos\end{bmatrix} \left(\frac{m\pi y}{a}\right) \mathrm{d}y \Bigg\}, \end{aligned}$$

where δ_{m0} is the Kronecker delta symbol. Next, we make the substitution $\eta = \pm(y - 2ja)$, where the upper and lower signs apply to the first and second integrals respectively. A small amount of manipulation now yields

$$A^1_m(x) = \frac{2}{(1+\delta_{m0})a} \int_0^{\infty} \phi_0(x, \eta) \begin{bmatrix}\sin\\ \cos\end{bmatrix} \left(\frac{m\pi \eta}{a}\right) \mathrm{d}\eta. \tag{13}$$

Finally, we substitute the general form of equation (1) for ϕ_0, and reverse the order of integration, to obtain

$$A^1_m(x) = \frac{1}{(1+\delta_{m0})a\pi} \int_{-\infty}^{\infty} \frac{S^+(\alpha)}{\gamma^{[\mp]}(\alpha)} \mathrm{e}^{-\mathrm{i}\alpha x} \int_0^{\infty} \mathrm{e}^{-\gamma(\alpha)\eta} \begin{bmatrix}\sin\\ \cos\end{bmatrix} \left(\frac{m\pi \eta}{a}\right) \mathrm{d}\eta\, \mathrm{d}\alpha.$$

Recalling that k has a small, positive imaginary part, we evaluate the integral in η to obtain

$$A^1_m(x) = \frac{1}{(1+\delta_{m0})a\pi} \int_{-\infty}^{\infty} \frac{S^+(\alpha)\,\mathrm{e}^{-\mathrm{i}\alpha x}}{\alpha^2 - \alpha_m^2} \begin{bmatrix}(m\pi)/(a\gamma^-)\\ \gamma^-\end{bmatrix} \mathrm{d}\alpha, \tag{14}$$

where

$$\alpha_m = \left[k^2 - \left(\frac{m\pi}{a}\right)^2\right]^{1/2} \qquad (m = 0, 1, \ldots).$$

This lies in the upper-right quadrant of the α plane. Note that, for sufficiently large m, (14) includes the possibility of evanescent modes, which decay exponentially with increasing x. These are only of significance close to the aperture, where they play a part in connecting the field within the guide to that outside; far inside the guide their effect on the field may be ignored. To determine ϕ^{u}, the field due to primary diffraction at the upper edge $(0, a)$, we introduce the coordinate transformation

$$\hat{y} = a - y. \tag{15}$$

In this case, we must not include the incident field, or its specular reflection from $y = a$; these have already been accounted for. However, since we are now on the lit side of the plane, in contrast to the situation for ϕ^{l} (cf discussion in section 2), the procedure remains identical, and the introduction of ϕ' (1) yields the correct result. The only differences in the expressions for ϕ^{u} and ϕ^{l} are that, in the latter case, the incident field must be written in terms of $\hat{y}$ (so S^+ will differ slightly), and a multiplicative factor of $[\mp](-1)^m$ must be included when the Fourier series is written in terms of y as opposed to $\hat{y}$. The field due to primary diffraction excited within the guide has now been expressed as an expansion using the permissible modes [6, 7] as a basis. The fact that we arrive at such a result acts as a useful check on the method we have used to obtain it.

4. Specific examples

We now calculate the modes excited within the waveguide by primary diffraction of three different incident fields.

4.1. External plane wave incidence

Suppose that the incident field is the plane wave

$$\phi^{\mathrm{i}}(x, y) = \mathrm{e}^{\mathrm{i}k(x\cos\Theta + y\sin\Theta)}.$$

Before performing the relevant calculations in this case, it is interesting to examine the behaviour of the plane waves within the guide. Thus, consider the situation shown in figure 2, where $\Theta \in \left[0, \frac{\pi}{2}\right)$. A similar argument can be applied if $\Theta \in \left(-\frac{\pi}{2}, 0\right)$; these are the only cases where the following behaviour occurs. Since ϕ_0 is the total field in the absence of the upper half-plane it contains the incident field, which is switched off to the right of the line $y = x\tan\Theta$, see figure 2. The image source ϕ_2 gives the reflection of this field, which is deactivated to the right of the line $y = 2a - x\tan\Theta$. Also, since ϕ_1 has had the reflected field subtracted, it contains a term which deactivates the plane wave from ϕ_2 to the left of $y = a - x\tan\Theta$. This process of activation and deactivation continues throughout the guide, so that the requirements of geometrical optics are satisfied.

The total field within the guide is easily calculated; since the contour of integration passes below the pole of S^+, which in this case is given by (14), the residue from the $\alpha = -\alpha_m$ is the only contribution. Thus, ϕ^{l} is given by (12), with

$$A_m^{\mathrm{l}}(x) = \begin{bmatrix} \cos\frac{\Theta}{2} \\ -\mathrm{i}\sin\frac{\Theta}{2} \end{bmatrix} \frac{\mathrm{e}^{\mathrm{i}\pi/4}\sqrt{2k}\,\gamma^{[\mp]}(\alpha_m)\,\mathrm{e}^{\mathrm{i}\alpha_m x}}{(1+\delta_{m0})a\alpha_m(k\cos\Theta - \alpha_m)}. \tag{16}$$

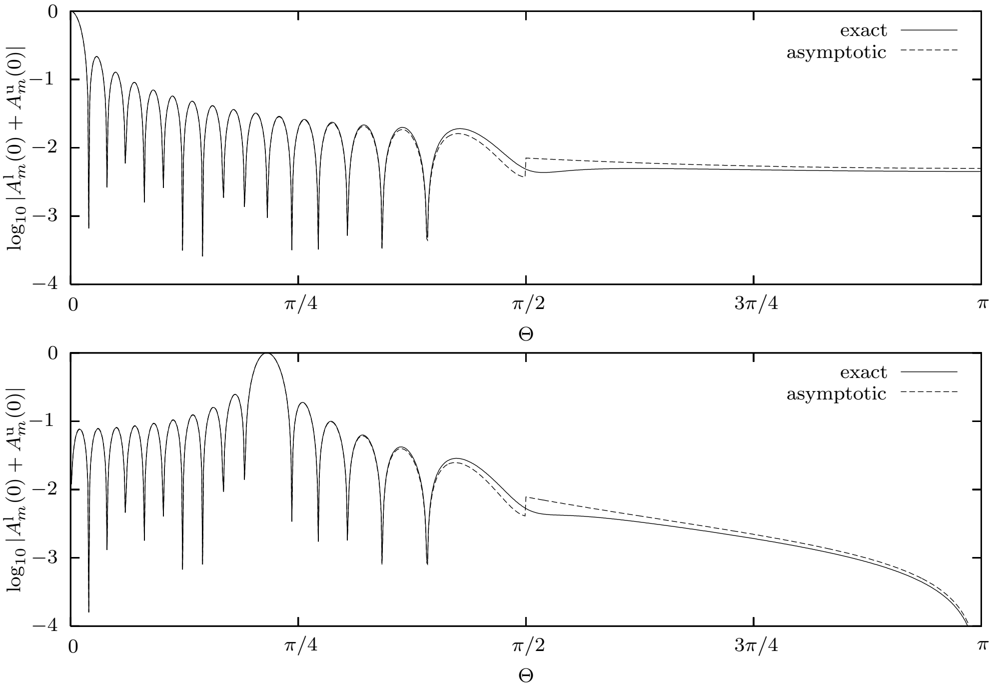

Figure 3. Logarithmic plots of the modal amplitude coefficients for varying angles of incidence, with $ka = 100$. Upper: Neumann case, $m = 0$; lower: Dirichlet case, $m = 20$.

The modes due to diffraction at the upper edge may also be expressed as a series of the form (12), with A^{l}_m replaced by A^{u}_m. Since

$$\phi^{\mathrm{i}}(x, \hat{y}) = \mathrm{e}^{\mathrm{i}ka\sin\Theta}\,\mathrm{e}^{\mathrm{i}k(x\cos\Theta - \hat{y}\sin\Theta)},$$

it follows that

$$A^{\mathrm{u}}_m(x) = (-1)^{m+1}\,\mathrm{e}^{\mathrm{i}ka\sin\Theta} A^{\mathrm{l}}_m(x). \tag{17}$$

Here, the additional '−' occurs in the Neumann case since Θ is replaced by $-\Theta$ in (3) to account for the downward propagating (in $\hat{y}$) incident field. As noted in the introduction, we have constructed the first term in an asymptotic expansion of the modal amplitude coefficients in the high-frequency limit; it is given by (16) multiplied by the factor $[1 - (-1)^m\,\mathrm{e}^{\mathrm{i}ka\sin\Theta}]$. This expansion breaks down if the width of the guide is close to a modal cutoff, which corresponds to $\alpha_m = 0$. Note that, in the Neumann case with $m = 0$, the limit $\Theta \to 0$ may be applied to $A^{\mathrm{l}}_m(x) + A^{\mathrm{u}}_m(x)$ using L'Hôpital's rule. It yields unity as we should expect, since in this special case the incident field itself (i.e. $\mathrm{e}^{\mathrm{i}kx}$) satisfies the boundary conditions, and enters the guide unaffected by the aperture. For this geometrically simple case, exact solutions may be calculated using the Wiener–Hopf technique [9]. Figure 3 compares the modulus of the exact modal amplitude coefficients with those calculated via (16) and (17) with $ka = 100$, for varying Θ. This shows the strength with which the mode in question is excited; secondary diffraction effects must be included in order to accurately approximate the phase of the coefficients [8]. The highest travelling (i.e. not evanescent) mode number, $m_{\max} = 31$; the figures are plotted for the $m = 0$ and $m = 10$ modes in the Neumann and Dirichlet cases respectively. Good agreement with the exact results is evident, particularly for $\Theta < \frac{\pi}{2}$. Note the differing behaviour of the coefficients for $\Theta \lessgtr \frac{\pi}{2}$, which is due to the presence or absence

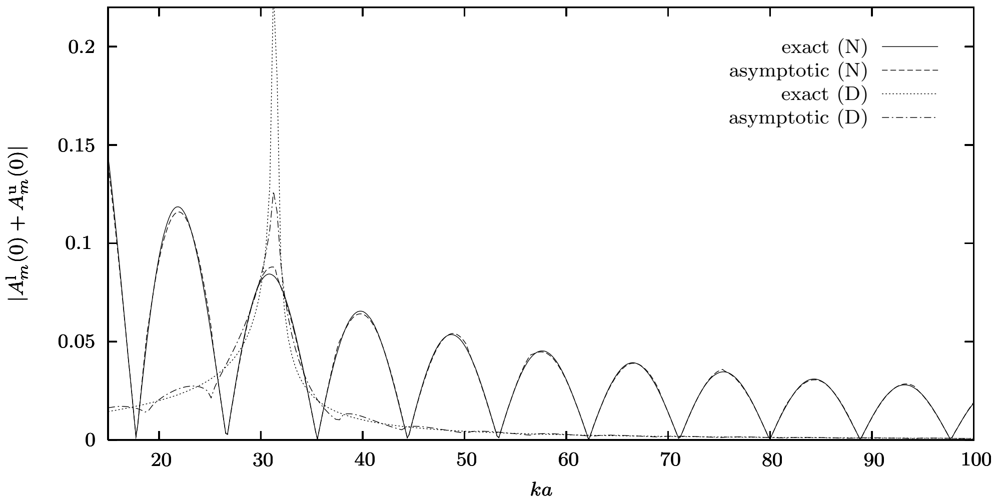

Figure 4. Modal amplitude coefficients for varying ka. (N): Neumann case, $m = 0$, $\Theta = \frac{\pi}{4}$; (D): Dirichlet case, $m = 10$, $\Theta = \frac{3\pi}{4}$.

of plane waves and their associated Fresnel regions in the interior of the guide. Also note the presence of a 'peak excitation angle' at which $A^{\mathrm{l}}_m(0) + A^{\mathrm{u}}_m(0) \approx 1$. Each travelling mode was found to possess one such angle; these become increasingly close to $\frac{\pi}{2}$ as $m \to m_{\max}$. Figure 4 shows the modal amplitude coefficients for varying ka with $\Theta = \frac{\pi}{4}$ and $m = 0$ in the Neumann case, and $\Theta = \frac{3\pi}{4}$ and $m = 10$ in the Dirichlet case. Once again, the different nature of the results for $\Theta \lesseqgtr \frac{\pi}{2}$ is clearly visible. Reasonable agreement between the exact and asymptotic results is evident, even for values as low as $ka \approx 20$. Note the breakdown of the asymptotic approximation in the vicinity of the modal cutoff in the Dirichlet case (the $m = 0$ mode in the Neumann case is present at all frequencies).

At this point it is of some interest to briefly examine the ray theory approach of Yee *et al* [8]. Although external wave incidence was not actually considered by these authors, their method may be applied provided that there are no Fresnel regions present within the guide, which is a significant limitation. Thus, we return to the integral (13) and replace ϕ_0 with its well-known leading-order asymptotic expansion [12], i.e.

$$\phi_0(x, \eta) \sim \frac{-\mathrm{e}^{\mathrm{i}kr}\mathrm{e}^{\mathrm{i}\pi/4}}{\sqrt{\pi k}(r\cos\Theta - x)} \begin{bmatrix} \cos\frac{\Theta}{2}\sqrt{r - x} \\ \sin\frac{\Theta}{2}\sqrt{r + x} \end{bmatrix},$$

wherein

$$r = \sqrt{x^2 + \eta^2}.$$

Note that we have used the fact that only $\eta > 0$ need be considered in converting from the standard polar form. After some manipulation, we now rewrite the Fourier coefficient A_m in (13) for ϕ^{l} in the form

$$A^{\mathrm{l}}_m(x) \sim \frac{-\mathrm{e}^{\mathrm{i}\pi/4}}{(1 + \delta_{m0})a\sqrt{\pi k}} \begin{bmatrix} \cos\frac{\Theta}{2}\mathrm{i}\,\mathrm{sgn}(\eta) \\ \sin\frac{\Theta}{2} \end{bmatrix} \int_{-\infty}^{\infty} \sqrt{r[\mp]x}\, \frac{\mathrm{e}^{\mathrm{i}k\chi(\eta)}}{r\cos\Theta - x}\,\mathrm{d}\eta,$$

where

$$\chi(\eta) = \sqrt{\eta^2 + x^2} - \frac{m\pi\eta}{ak}.$$

Now the stationary phase approximation of this integral requires some liberties to be taken with the method, since χ depends upon k, and the relative size of $m\pi/a$ varies for different modes. Allowing for this, it is not difficult to see that there is a first-order saddle located at the point $\eta = \eta_{\mathrm{s}}$, where

$$\eta_{\mathrm{s}} = m\pi x/(\alpha_m a).$$

Interestingly, the contribution from this saddle point turns out to be identical to the exact result (16), as is easily shown for travelling modes using the standard formula [15].

4.2. Travelling mode incidence from within the guide

Suppose now that the incident field is the nth left travelling mode, which may be written in terms of plane waves as

$$\phi^{\mathrm{i}}(x, y) = \frac{1}{2}\begin{bmatrix}\mathrm{i}\\1\end{bmatrix}(\mathrm{e}^{\mathrm{i}k(x\cos\Theta+y\sin\Theta)}[\mp]\,\mathrm{e}^{\mathrm{i}k(x\cos\Theta-y\sin\Theta)}), \tag{18}$$

with

$$\cos\Theta = -\frac{\alpha_n}{k}, \qquad \sin\Theta = -\frac{n\pi}{ak}. \tag{19}$$

This implies that $\Theta \in \left(-\pi, -\frac{\pi}{2}\right)$, therefore the first term in (18) represents a downward propagating plane wave, and the second term its specular reflection from $y = 0$. Hence, we calculate ϕ^{l} as the diffraction of the first term from $(0, 0)$, and ϕ^{u} as that of the second from $(0, a)$. In the former case, we obtain

$$A_m^{\mathrm{l}}(x) = \begin{bmatrix}-\cos\frac{\Theta}{2}\\ \sin\frac{\Theta}{2}\end{bmatrix}\frac{\mathrm{e}^{-\mathrm{i}\pi/4}\sqrt{k/2}\gamma^{[\mp]}(\alpha_m)\,\mathrm{e}^{\mathrm{i}\alpha_m x}}{(1+\delta_{m0})a\alpha_m(k\cos\Theta-\alpha_m)}, \tag{20}$$

and for the latter we find that

$$A_m^{\mathrm{u}}(x) = (-1)^m\,\mathrm{e}^{-\mathrm{i}ka\sin\Theta}A_m^{\mathrm{l}}(x). \tag{21}$$

Using relations (19), and combining the two results yields the total field within the guide to leading order, thus

$$\phi^{\mathrm{t}}(x, y) = \sqrt{k[\mp]\alpha_n}\begin{bmatrix}\sin\\ \cos\end{bmatrix}\left(\frac{m\pi y}{a}\right)\frac{\mathrm{e}^{-\mathrm{i}\pi/4}\gamma^{[\mp]}(\alpha_m)\,(1+(-1)^{m+n})}{(1+\delta_{m0})2a\alpha_m(\alpha_n+\alpha_m)}\,\mathrm{e}^{\mathrm{i}\alpha_m x}.$$

This result is in agreement with Yee *et al* [8] in the Dirichlet case. In the Neumann case, it is consistent with the results of Boersma [11]; here Yee *et al* appear to have included an erroneous factor of $\frac{1}{2}$. An earlier attempt at performing the calculation in this case was made by Ciarkowski [16]; this work appears to be incorrect as it does not seem to account for the specular reflections that occur within the guide. Various numerical results for this type of incident field are available; see [8, 11].

4.3. Cylindrical wave incidence from free space

In this case, S^{+} is replaced by $-S^{-}$ (10) in (14), as noted in section 2. The field in the guide follows immediately; thus, ϕ^{l} is again given by (12), with

$$A_m^{\mathrm{l}}(x) = \begin{bmatrix}1\\ -\mathrm{i}\,\mathrm{sgn}(Y)\end{bmatrix}\frac{\mathrm{e}^{\mathrm{i}kR}\,\mathrm{e}^{\mathrm{i}\alpha_m x}}{(1+\delta_{m0})4a\alpha_m}[w(-z_1)[\mp]w(z_2)], \tag{22}$$

where z_1 and z_2 are given by equations (6) and (6), with $\alpha = -\alpha_m$. Some care must be taken when calculating ϕ^{u}, since, unlike the case of plane waves, the parameter Θ changes on introduction of $\hat{y}$ (cf equation (15)) here. Thus, the usual multiplicative factor of $[\mp](-1)^m$ must be included when the Fourier series is written in terms of y, and in addition, we must introduce new Cartesian and polar coordinates for the source location in the $(x, \hat{y})$ plane. Therefore, we write

$$\hat{Y} = -(Y + a), \qquad \hat{R} = \sqrt{X^2 + \hat{Y}^2},$$

so that the position of the line source is now defined by the relations

$$\hat{R}\cos\hat{\Theta} = X, \qquad \hat{R}\sin\hat{\Theta} = \hat{Y}.$$

The source coordinates in (22) are now replaced with circumflexed parameters to yield ϕ^{u}. Thus, the Fourier coefficients of the field within the guide are given to leading order by (22), added to

$$A_m^{\mathrm{u}}(x) = \begin{bmatrix} -1 \\ \mathrm{i}\,\mathrm{sgn}(Y + a) \end{bmatrix} \frac{(-1)^m\, \mathrm{e}^{\mathrm{i}k\hat{R}}\, \mathrm{e}^{\mathrm{i}\alpha_m x}}{(1 + \delta_{m0}) 4a\alpha_m} [w(-\hat{z}_1)[\mp]w(\hat{z}_2)],$$

where the circumflexed values z_1 and z_2 are obtained from (6) and (6) on replacement of R with $\hat{R}$.

Finally, we remark that in the limit $R \to \infty$, the leading-order term in the asymptotic expansion of the Hankel function [9] can be used to show that

$$\phi^{\mathrm{i}}(x, y) \sim c\, \mathrm{e}^{\mathrm{i}k(x\cos\Theta + y\sin\Theta)},$$

wherein

$$c = \frac{-\mathrm{e}^{\mathrm{i}\pi/4}\, \mathrm{e}^{\mathrm{i}kR}}{2\sqrt{2\pi kR}}.$$

Taking the same limit in (22), using expansion (8) and dividing by c, we therefore retrieve (16). For diffraction from the upper half-plane, note that we must still take $R \to \infty$ (and not $\hat{R}$), so that the angle of incidence tends to the same limit at both of the half-planes; the factor c does not change. The signum function in (22) then yields a multiplicative factor $[\pm]$, and the phase difference observed in section 4.1 is obtained from the limit

$$\lim_{R\to\infty} \mathrm{e}^{\mathrm{i}k\hat{R}}\, \mathrm{e}^{-\mathrm{i}kR} = \mathrm{e}^{\mathrm{i}ka\sin\Theta}.$$

Hence, we can retrieve the plane wave case as an appropriate limit of the cylindrical wave incidence problem, a useful check on the accuracy of our results. To present numerical results in this case, it is simplest to assume that the equations are scaled so that $a = 1$. Figure 5 shows modal amplitude coefficients for a source whose position is given by $X = 100$, with varying Y. In the upper plot where $-1 \leqslant Y \leqslant 0$, the interior of the guide is in a direct 'line of sight' from the source position; this type of incident field has no equivalent in terms of plane waves. The strength with which the mode is excited oscillates as Y varies; the frequency of these oscillations is greater for higher modes. As we should expect, this plot is symmetric about $Y = 0.5$. In the lower plot, $Y > 0$, and the response to the plane wave $c\,\mathrm{e}^{\mathrm{i}k(x\cos\Theta + y\sin\Theta)}$ is shown for comparison. Again, a peak excitation angle is evident for both modes, though it is considerably weaker than the strong excitations that are possible for $-1 \leqslant Y \leqslant 0$.

5. Concluding remarks

We have retrieved the results of Yee *et al* [8] for primary diffraction at the aperture of a waveguide bounded by half-planes without resorting to any approximations, and our development is applicable to both internal and external wave incidence upon the aperture. In particular, we have calculated the amplitude coefficients of modes generated by the diffraction

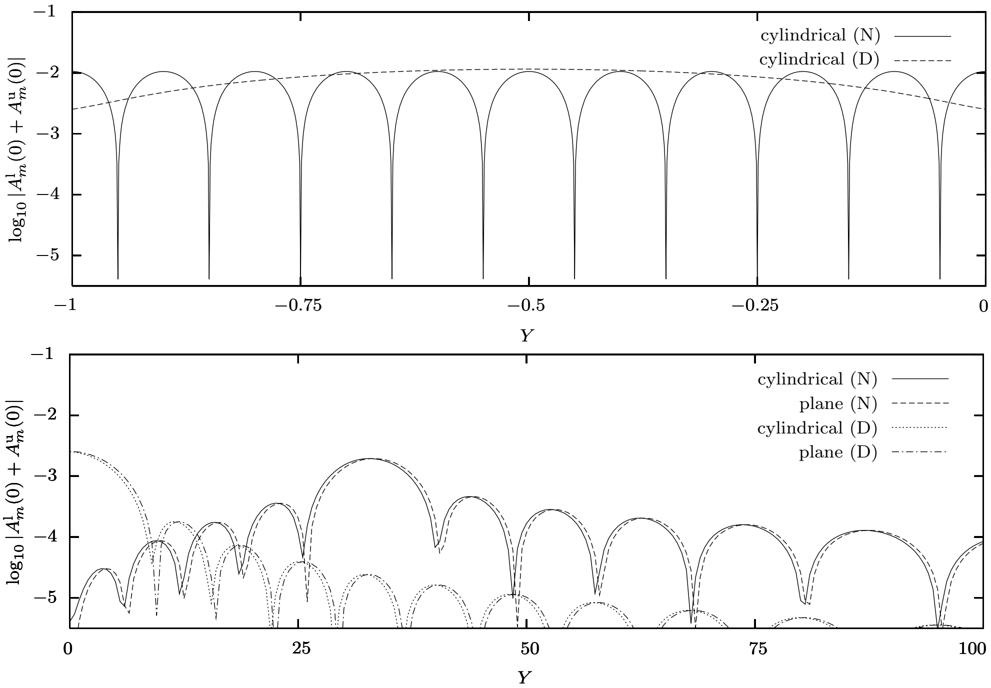

Figure 5. Modal amplitude coefficients for $k = 100$, $X = 100$ with varying Y. (N): Neumann case, $m = 10$, (D): Dirichlet case, $m = 1$.

of waves emanating from an external line source to leading order in the high-frequency limit; this would be difficult to obtain by other means. The accuracy of these leading-order asymptotics is supported by numerical results, which show that the coefficients remain accurate for moderate frequencies. Since our analysis involves exact evaluation of integrals derived from those representing diffraction by a half-plane, and because these integrals automatically take account of features such as geometrical shadow and reflection boundaries, it has not been necessary to take special notice of such effects.

Straightforward extensions to the method used here include the consideration of staggered plates, mixed boundary conditions and guides of finite length. One might also attempt to consider three-dimensional problems in which the waveguide is finite in the z direction. This is likely to prove difficult, however, as it introduces corner effects, and prevents the use of methods involving half-plane diffraction integrals such as that employed here.

Acknowledgments

This work was supported by an EPSRC Faraday Award, grant reference GR/R93445/01. The authors are grateful for useful collaborative discussions with Dr E Davenport (BAE SYSTEMS), Dr D Ward, Dr A Ruddle (MIRA) and Dr D J Allwright (Smith Institute).

References

[1] Keller J B 1962 Geometrical theory of diffraction *J. Opt. Soc. Am.* **52** 116–30

[2] Keller J B and Lewis R M 1995 Asymptotic methods for partial differential equations: The reduced wave equation and Maxwell's equations *Surveys in Applied Mathematics* (New York: Plenum) pp 1–82
[3] Anile A M, Hunter J K, Pantano P and Russo G 1993 Ray methods for nonlinear waves in fluids and plasmas vol 57 *Pitman Monographs and Surveys in Pure and Applied Mathematics* Longman Scientific and Technical (New York: Wiley)
[4] Prasad P 1994 A nonlinear ray theory *Wave Motion* **20** 21–31
[5] Keller J B and Rubinow S I 1960 Asymptotic solution of eigenvalue problems *Ann. Phys.* **9** 24–75
[6] Saleh B E A and Teich M C T 1991 *Fundamentals of Photonics* (New York: Wiley)
[7] Billingham J and King A 2000 *Wave Motion* (Cambridge: Cambridge University Press)
[8] Yee H Y, Felsen L B and Keller J B 1968 Ray theory of relection from the open end of a waveguide *SIAM J. Appl. Math.* **16** 268–300
[9] Noble B N 1988 *Methods Based on the Wiener-Hopf Technique* (New York: Chelsea)
[10] Bowman J J 1970 Comparison of ray theory with exact theory for scattering by open waveguides *SIAM J. Appl. Math.* **18** 818–29
[11] Boersma J 1975 Ray-optical analysis of reflection in an open-ended parallel-plane waveguide. I: TM case *SIAM J. Appl. Math.* **29** 164–95
[12] Bowman J J, Senior T B A and Uslenghi P L E 1969 *Electromagnetic and Acoustic Scattering by Simple Shapes* (Amsterdam: North-Holland)
[13] Jones D S 1964 *The Theory of Electromagnetism* (Oxford: Pergamon)
[14] Abramowitz M and Stegun I 1965 *Handbook of Mathematical Functions* (New York: Dover)
[15] Murray J D 1974 *Asymptotic analysis* (Oxford: Clarendon)
[16] Ciarkowski A 1975 An application of uniform asymptotic theory of diffraction by a plane screen to the analysis of an open-ended waveguide *Acta Phys. Polonica* A **47** 621–31